RSC Advances

ROYAL SOCIETY
OF CHEMISTRY

www.rsc.org/advances
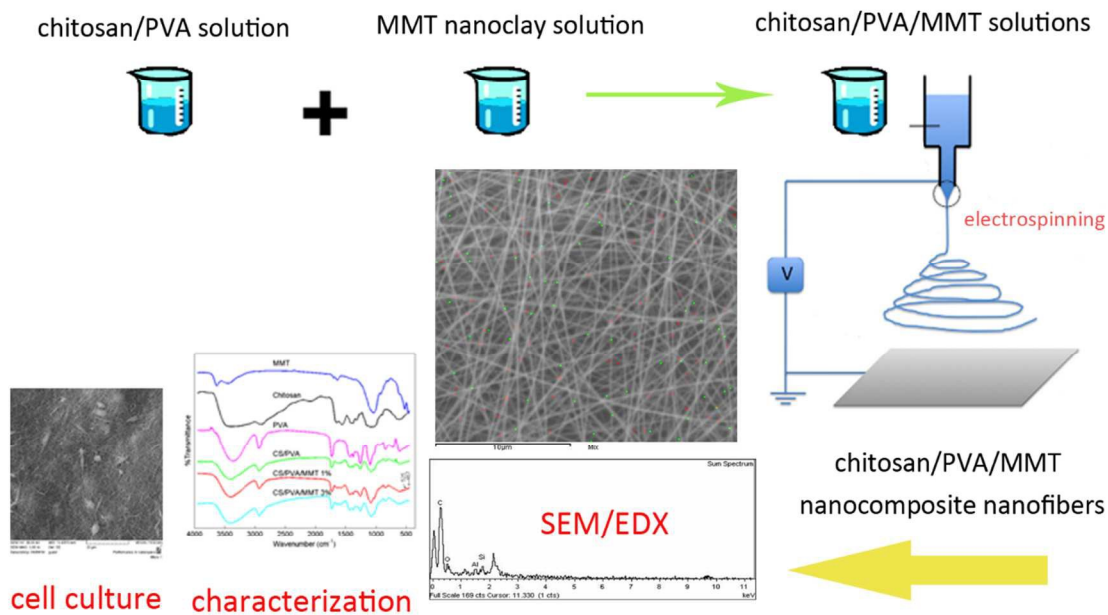
Chitosan/PVA/nanoclay nanocomposite nanofibers have been prepared successfully by electrospinning. Bead-free morphology was achieved for the nanofibrous mats and the nanoclays were incorporated and distributed uniformly inside the nanofibers.

Nanoclay-reinforced electrospun chitosan/PVA nanocomposite nanofibers for biomedical applications

Mojtaba Koosha [a], Mohammad Ali Shokrgozar [b], Hamid Mirzadeh [a,*], Mehdi Farokhi [b]

[a] Department of Polymer Engineering and Color Technology, Amirkabir University of Technology (Tehran Polytechnic), 424 Hafez Avenue, Tehran, Iran. mkoosha@aut.ac.ir, mirzadeh@aut.ac.ir

[b] National Cell Bank of Iran, Pasteur Institute of Iran, Tehran, Iran. mashokrgozar@pasteur.ac.ir , mehdifarokhi83@gmail.com

[*] Corresponding author. E-mail: mirzadeh@aut.ac.ir ; tel: +982164542420

Abstract

Nanofibrous nanocomposites based on chitosan/poly (vinyl alcohol) blend and Na-montmorillonite (MMT) nanoclays were prepared by the electrospinning technique. The morphological studies of the electrospun mats revealed that uniform bead-free nanofibers were formed. Existence of MMT in the nanofibrous mats were approved by FTIR and energy dispersive X-ray Scattering (EDX). The high aspect ratio MMT nanoclays were incorporated inside the nanofibers. Small angle X-ray diffraction (SAXRD) measurements showed that the electrospinning process has significantly affected the interlayer spacing of the nanoclays. Incorporation of nanoclays into the nanofibers enhanced the tensile strength and increased the glass transition of the mats. The cytotoxicity of nanocomposite mats was examined by MTT assay using A-431 cell line. The clay-containing nanofibrous mats did not show any significant effect on the viability of the cells. The A-431 cells were properly attached on the surface of the mats.

Keywords: Chitosan; Poly(vinyl alcohol); Nanoclay; Cytotoxicity; Nanocomposites; Nanofibers;

1 Introduction

Polymer layered silicate nanocomposites technology is widely used to enhance properties of polymers by incorporation of nanoclays into the matrix. Montmorillonite (MMT) is a 2:1 type of aluminosilicate with a layered structure which is used as nanofiller for preparation of polymer layered silicate nanocomposites in many works [1-3]. Dispersion of nanoclays into the polymer matrices is performed through melt or solution intercalation and is of great importance in determining the final physical and mechanical properties of the nanocomposites [4]. Electrospinning is one of the best techniques for production of nanofibers from polymers, composites and ceramics [5]. In this process, the conductive polymer solution flows through a needle and by applying an external electric field, the viscoelastic fluid is elongated leading to formation of a jet [6]. Electrostatic repulsion between surface charges and solvent evaporation reduces the diameter of the jet leading to ultrafine nanoscale fibers. The nanofibrous structures produced by electrospinning have characteristics such as high surface area to volume ratio and high porosity [5]. Many polymers have been electrospun to nanofibers successfully[7-9]. Electrospinning is one of the most efficient methods to incorporate nanoparticles into polymer matrices and is used for incorporation of nanoparticles into nanocomposite materials [10]. High voltage electric field and the elongational flow in the electrospinning process can enhance the dispersion of nanoparticles [11]. Production of nanofibers containing nanofillers can enhance physical and mechanical properties of the electrospun mats.

Chitin and specially its deacetylated form, chitosan, are biocompatible, biodegradable and non-toxic biopolymers that are widely used in biomedical applications such as tissue engineering, wound healing and dressings, drug delivery systems and separation membranes [12, 13]. In our pervious study, we fabricated chitosan/ polyvinyl alcohol (PVA) nanofibers reinforced by single-walled carbon nanotube for potential use in neural tissue engineering by electrospinning method [14]. Solution intercalated chitosan/MMT nanocomposites have been prepared by mechanical mixing in many works[15, 16]. However, few studies are

available on the incorporation of MMT nanoclays into chitosan nanofibers and its effect on physical, mechanical and biocompatibility of the mats. Park and coworkers have prepared nanocomposite nanofibers from PVA, chitosan oligosaccharides and MMT nanoclays [17]. They considered the morphology, tensile strength and thermal properties of the mats but the cell behavior and cytotoxicity of the mats were not studied. In another work, organic rectorite (OREC) which is a type of synthetic silicate nanolayer with a larger interlayer distance and easily separable layers, was used to fabricate chitosan/PVA/OREC and quaternized chitosan/PVA/OREC nanocomposite nanofibers[18-20]. They have studied the antibacterial activity of mats, while the mechanical properties and cytotoxicity of the electrospun nanocomposite mats have not been considered. Similarly, fabrication of carboxymethyl chitin/OREC nanofibrous mats showed that presence of OREC induces a small cytotoxicity to the fibroblast cells [21].

To the best of our knowledge, there is not any work available on the electrospinning of chitosan solutions containing natural montmorillonite nanoclays. Furthermore, the mechanical properties and *in vitro* cytotoxicity have not been considered in the previous works, clearly. In this study, electrospinning was used to prepare chitosan/PVA/MMT nanocomposite nanofibers. To produce nanofibers, PVA was used as the guest polymer because of its high miscibility and favorable interactions with chitosan in the molecular level [22] . Acetic acid/Water mixture was used as solvent and MMT nanolayers are mixed with chitosan/PVA solutions and electrospun into nanofibers. Morphology of the nanofibrous mats are studied by scanning electron microscope (SEM). The mechanical and thermal properties of the electrospun mats were characterized by tensile strength, dynamic mechanical thermal analysis (DMTA) and differential scanning calorimetry (DSC) experiments. Biocompatibility assay is performed to study the cytotoxicity of the nanocomposite mats and human fibroblast (A-431 cell line) cell behavior is considered.

3

2 Results

2.1 Morphology of nanocomposite nanofibers and distribution of nanoclays by SEM/EDX

SEM micrographs of nanofibrous membranes electrospun form CS/PVA and CS/PVA/MMT solutions containing 1 and 3% nanoclays are shown in figure 1 (a-c). Uniform bead-free morphology is observed for the electrospun nanofibers of CS/PVA, CS/PVA/MMT 1% and CS/PVA/MMT 3%. Average diameters of nanofibers are presented in Table 1. It is seen that average diameters of nanofibers are decreased by increasing the nanoclay content in the solutions. The difference between the diameters of CS/PVA and CS/PVA/MMT 1% are not significant while the sample CS/PVA/MMT 3% has a significantly lower diameter with a narrower fiber size distribution comparing to the other samples. Similar result was observed by other researchers 11 for PCL/clay nanofibers but the difference between the sizes were not significant. However, in our work the diameters of nanofibers were decreased by increasing the MMT content to 3% because according to the method used for solution intercalation of nanocomposites, for preparation of the sample CS/PVA/MMT 3% more solvent is added to the solution which results in a decrease in the viscosity of the solution and leads to the reduction of fiber diameters.

Sample	Average Fiber Diameter (nm)
CS/PVA	190 ±34
CS/PVA/MMT 1%	205 ±93
CS/PVA/MMT 3%	135 ±23

Table 1 Average diameters of nanofibers electrospun from solutions of chitosan/PVA containing 1 and 3% MMT measured from the SEM images.
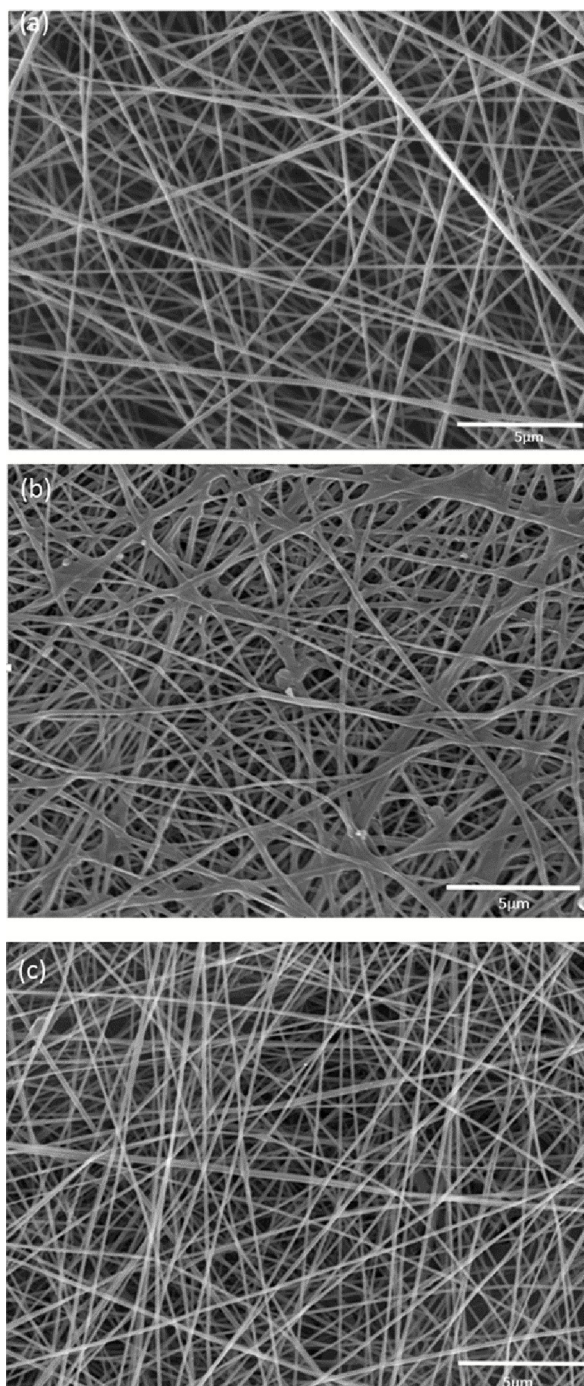
4

Figure 1- Scanning electron micrographs of CS/PVA (a), CS/PVA/MMT 1% (b), and CS/PVA/MMT 3% (c) electrospun nanocomposite nanofibers (voltage 20 KV, TCD 10 cm, rate 0.1 ml/h).

5

In order to approve the presence of nanoclays inside the nanofibers, Al and Si elements, which only comprise the nanoclay structures, are mapped and the EDX spectrum is obtained. As is shown in figure 2 (b,c), the characteristic peaks of Al and Si elements are detected in the EDX spectrum which confirms the presence of nanoclays inside the nanofibrous structures. Furthermore, regarding to distribution of Al and Si elements, it was shown that the nanoclays were uniformly distributed inside the nanofibers.
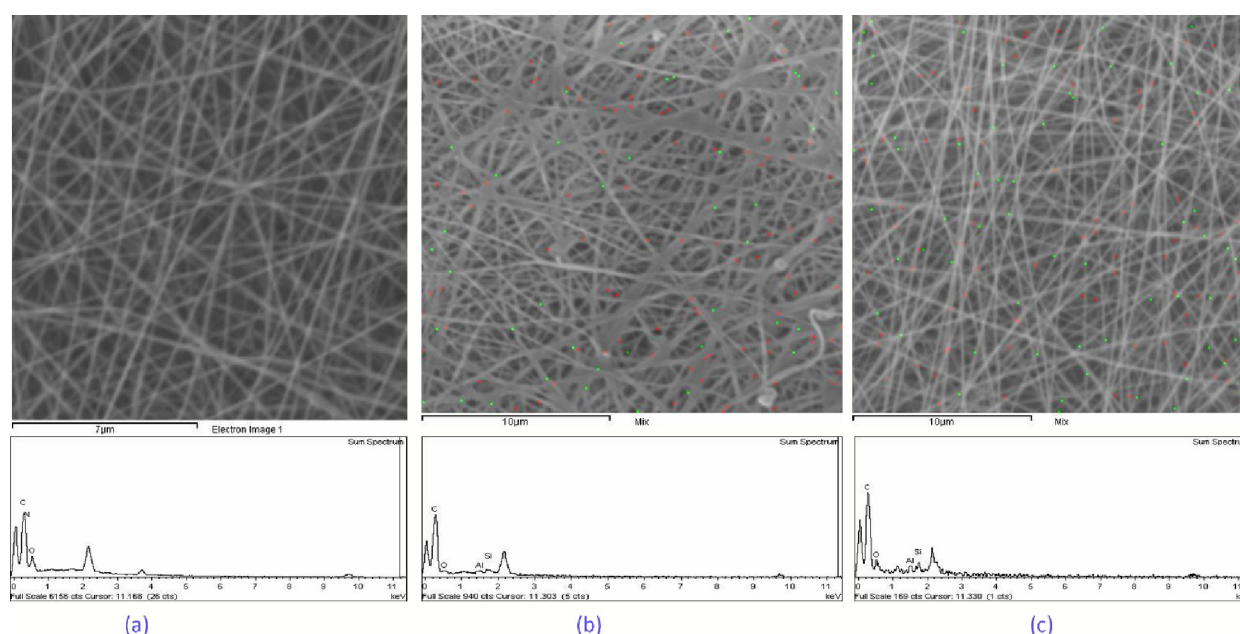
Figure 2- Mapping and spot analysis of the nanofibrous mats of CS/PVA (a), CS/PVA/MMT 1% (b) and CS/PVA/MMT 3% (c) obtained by energy dispersive X-ray scattering (EDX). (• Si, • Al).

2.2 FTIR spectroscopy

Figure 3 shows the FTIR spectra for as received MMT, chitosan, PVA and electrospun nanofibrous mats. Characteristic peaks of MMT, chitosan and PVA are tabulated in Table 2. MMT exhibits the four types of vibrations for Si-O and OH bonds (467, 525, 918, 3626, 1040 and 1635 cm^{-1}) which is in agreement with the literature data [2]. The chitosan spectrum showed the vibrations of primary and secondary amino

groups (3400 and 1602 cm^{-1}). Chitosan is obtained by deacetylation of chitin by alkaline treatment in a harsh environment and the acetamide groups transform into amine groups. The degree of deacetylation (DD) of the chitosan used in this study was calculated to be 92% [23].

In the case of PVA, all major peaks associated with hydroxyl acetate and acetate groups were observed. In fact, PVA is produced by alkaline treatment of poly (vinyl acetate) and is a copolymer of poly (vinyl alcohol-co-vinyl acetate). Although the PVA with 98% degree of hydrolysis was used in this study, 2% of acetate groups remain unhydrolyzed in the material. The peak at 1734 cm^{-1} is related to stretching vibrations of C=O groups of the remaining vinyl acetate repeat units in the PVA.
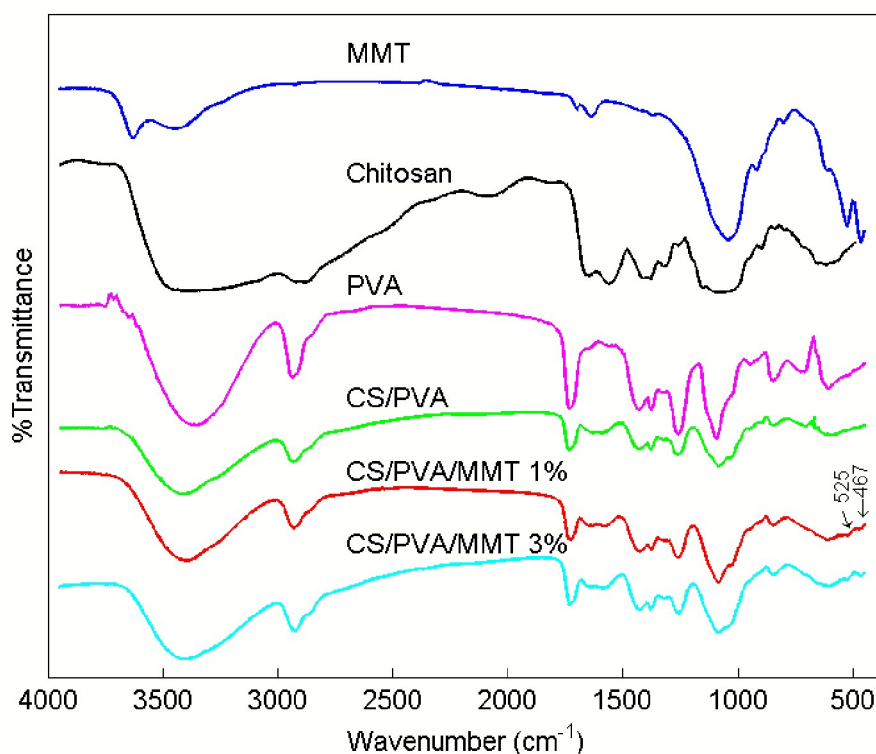

Figure 3- FTIR spectra of as-received MMT, chitosan and PVA and the electrospun nanofibrous mats CS/PVA, CS/PVA/MMT 1% and CS/PVA/MMT 3%.

7

MMT		Chitosan		PVA	
Wavenumber (cm^{-1})	Chemical Group	Wavenumber (cm^{-1})	Chemical Group	Wavenumber (cm^{-1})	Chemical Group
467 , 525	Si-O bending	3400	N-H stretching	3362	O-H
918 , 3626	OH vibration	1602	N-H deformation	2940	CH_2
1040	Si-O stretching	1648	C=O stretching	1734	C=O vibration
1635	H_2O Bending	1069	C-O stretching	1260	C-O stretching
		890	Ring stretching	1095	C-O-C
				845	C-C

Table 2 Characteristic FTIR peaks of MMT, chitosan and PVA and the relevant chemical groups.

FT-IR spectra of CS/PVA, CS/PVA/MMT 1% and CS/PVA/MMT 3% are also presented in figure 3. The spectra of the nanofibrous mats include the major characteristic peaks of both polymers. The peak at 3400 cm^{-1} is related to overlapping NH and OH stretching vibrations in chitosan and PVA comparing the spectrums of CS/PVA and CS/PVA MMT 1% in figure 3. The major absorptions at 467 $^{-1}$ and 525 cm^{-1} were observed in the spectrum of pure MMT, CS/PVA MMT 1% and CS/PVA MMT 3%, while these peak were absent in the spectrum of chitosan/PVA neat nanofibers. This result, in agreement with the EDX data, is another indication of the presence of MMT nanoclays inside the nanofibrous mats.

8

2.3 Small angle X-ray diffraction analysis

To investigate the gallery distance of MMT before and after electrospinning, small angle X-ray diffraction of the pristine MMT, CS/PVA and CS/PVA/MMT nanofibrous nanocomposites containing 1 and 3% MMT were recorded (figure 4). As shown, the interlayer distance for MMT calculated from the Bragg's equation is 1.17 nm. From figure 4, it can be seen that there is not any peak present for the samples CS/PVA, CS/PVA/MMT 1% and CS/PVA/MMT 3% in the scanned range. This result confirms that the MMT nanoclays are completely exfoliated inside the nanofibrous structures.
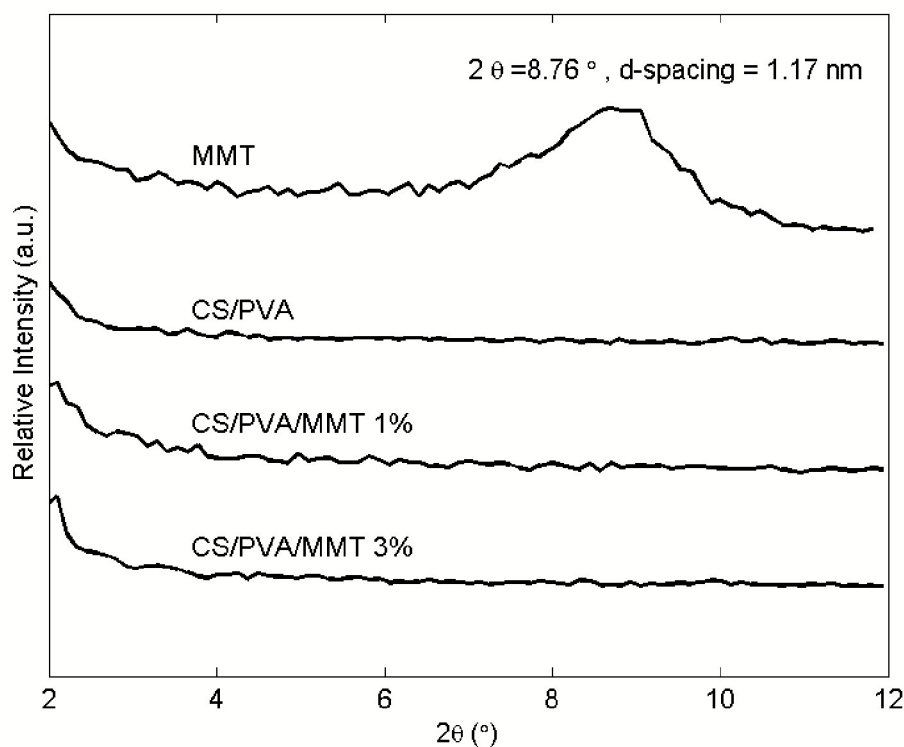

Figure 4- Small angle X-ray scattering of pristine MMT and the electrospun CS/PVA, CS/PVA/MMT 1% and CS/PVA/MMT 3% nanocomposite nanofibers.

2.4 DSC thermograms

DSC measurements can provide valuable data on phase transitions inside materials. Glass transition and melting are two important phenomena in polymers which are affected by processing conditions and additives in the materials [24]. DSC thermograms of MMT, chitosan and PVA and the resulting nanofibrous mats are presented in Figure 5. The first endothermic peak on the DSC curves of MMT and chitosan is assigned to the evaporation of bound water. The glass transition temperature of PVA is detected by a shift in baseline with an endothermic peak at 56°C. The melting temperature of PVA is found to be 190°C.

The glass transition of chitosan/PVA and chitosan/PVA/MMT 1% are found at around 52°C located inside an endothermic peak which is continued to 120°C related to the evaporation of water and acetic acid solvents. In the case of chitosan/PVA/MMT 3%, the position of this peak is shifted toward lower temperatures and the glass transition peak is not detected.
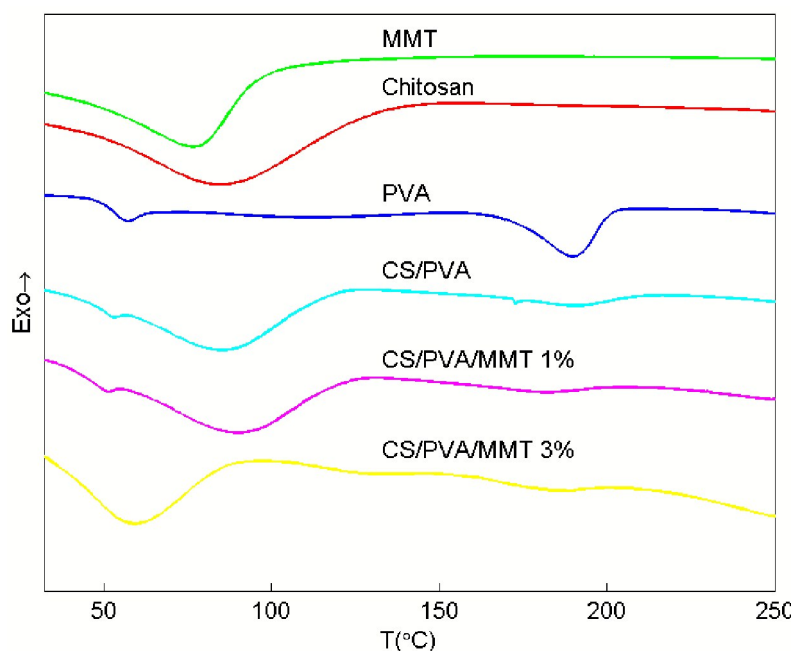

Figure 5- DSC thermograms of as-received MMT, chitosan and PVA as well as electrospun CS/PVA, CS/PVA/MMT 1% and CS/PVA/MMT 3% nanocomposite nanofibers.

10

In the DSC curves of the nanofibrous mats, a weak endothermic peak is found near 190°C which is due to melting of PVA crystals. The results show that glass transition and melting point of the pure PVA in the nanofibrous mats did not change significantly by presence of nanoclays.

2.5 Mechanical properties

2.5.1 Tensile strength

The tensile properties of the nanofibrous nanocomposite mats are presented in Table 3. Young's modulus, ultimate tensile strength (UTS), elongation at break (ε_b) and toughness of the mats are measured from the graphs of tensile strength test. The Young's moduli of the mats containing 1 and 3% nanoclay are significantly increased in comparison with the mat without nanoclay. By increasing the MMT content from 1 to 3% in the nanofibrous mats, the Young's modulus is decreased. The same trend can be observed for the values of ultimate tensile strength. In comparison to the CS/PVA, the elongation at break is decreased for CS/PVA MMT 1% while it is increased for CS/PVA/MMT 3%. From the data of table 3 it is observed that toughness is increased by increasing the nanoclay content in the mats.

sample	E (MPa)	UTS (MPa)	ε_b (%)	Toughness (MJ/m^3)
CS/PVA	190 ±37	5.26 ±0.53	4.5 ±1.3	0.153 ±0.05
CS/PVA/MMT 1%	858 ±53	15.45 ±0.95	2.7 ±0.2	0.260 ±0.03
CS/PVA MMT 3%	648 ±32	15.10 ±0.67	6.2 ±0.4	0.655 ±0.09

Table 3 Young's modulus (E), ultimate tensile strength (UTS), elongation at break (ε_b) and toughness of the nanocomposite nanofibrous mats.

11

2.5.2 DMTA results

Figure 6 (a,b) represents the dynamic mechanical behavior of chitosan/PVA nanofibrous mats with and without MMT. Temperature dependence of the storage moduli of the samples are shown in Figure 6a. The storage moduli of the nanocomposite nanofibers CS/PVA/MMT 1% and 3% show much higher values than that of CS/PVA over the entire temperature range of the experiment which is in agreement with the tensile strength of the mats. The storage modulus of the sample CS/PVA/MMT 3% is higher than the CS/PVA/MMT 1% over the temperatures less than 85°C and the values are overlapped above this temperature. An upturn in the storage modulus typical for the nanocomposite materials can be observed for the sample CS/PVA MMT 3%. An increase in the storage modulus is found in the temperature range of 20-70°C for the CS/PVA nanofibrous mat which is related to the evaporation of bound water.
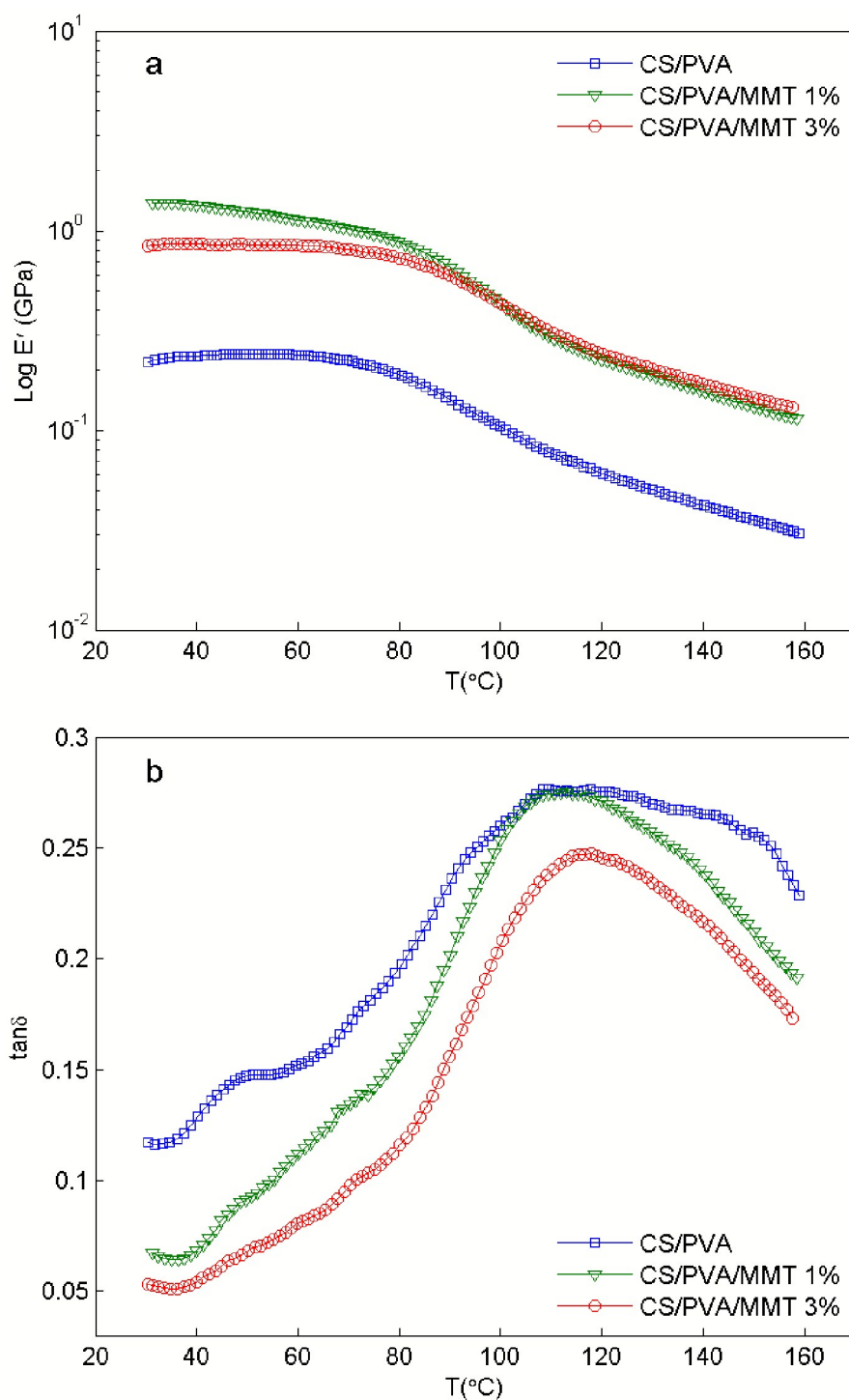
Figure 6- Storage modulus (a) and loss tangent (b) of the CS/PVA, CS/PVA/MMT 1% and

CS/PVA/MMT 3% nanocomposite nanofibrous mats as a function of temperature.

Figure 6b shows the variations of loss tangent (tan δ) with temperature for the nanocomposite samples. The tan δ peaks in the glass transition regions of the CS/PVA/MMT 1% and CS/PVA/MMT 3% have shifted to higher temperatures. This result indicates that the segmental motion of the polymer chains in the matrix is retarded by the layers of nanoclays. It is also notable that increasing the nanoclay content in the mats has lowered the values of loss tangent.

2.6 Cytotoxicity

The cell viability of human fibroblast cell line (A-431) was used to evaluate the cytotoxicity of the mats. Chitosan/PVA/MMT nanofibers, prepared in this study, are considered for biomedical applications as well as skin tissue engineering. The fibroblast cells are the major cells which are located in the skin tissue. For this reason we chose A-431 cell line because these cells are human derived with good proliferation rate. The percentage of cell viability for the nanofibrous nanocomposites using indirect MTT assay by culturing the cells with the extraction media of the mats after three incubation time intervals (1, 3 and 6 days) are presented in figure 7. According to the statistical analysis, the cell viabilities of the electrospun nanocomposite mats do not show any significant change in comparison to the control. All the samples showed cell viability greater than 90% in accordance to the control extraction media. This result confirmed that at the concentration of MMT nanoclays used for preparation of CS/PVA nanofibers, no adverse cytotoxic effect was detected.
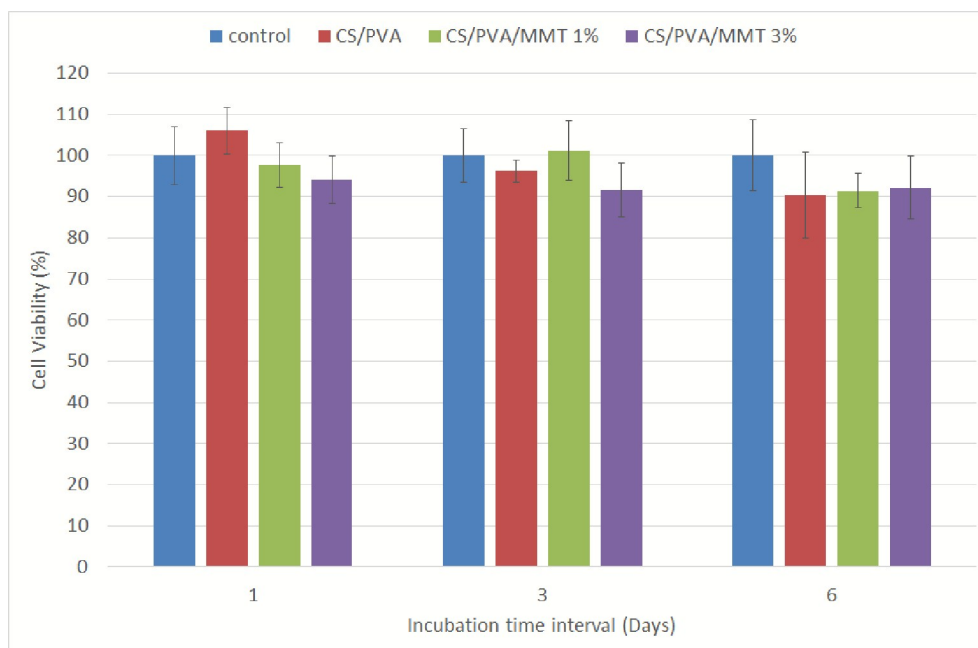
Figure 7- Cell viability of A431 cells in the extraction media obtained from immersion of the nanofibrous mats in the serum free RPMI medium for 1, 3 and 6 days.

2.7 Cell attachment study

The SEM micrographs of A-431 cells seeded on the surface of the thermally stabilized nanocomposite nanofibers are presented in figure 8. Cell attachment study was performed for CS/PVA, CS/PVA/MMT 1% and CS/PVA/MMT 3% nanocomposite mats. The SEM micrographs revealed that the electrospun nanocomposite nanofibers had porous surfaces with suitable pore size which allowed the cells to adhere to the surface of the mats with proper morphology.

15

Figure 8- Scanning electron micrographs of A431 cells attached on the surface of the nanocomposite mats (a) CS/PVA, (b) CS/PVA/MMT 1%, (c) CS/PVA/MMT 3%.

3 Discussion

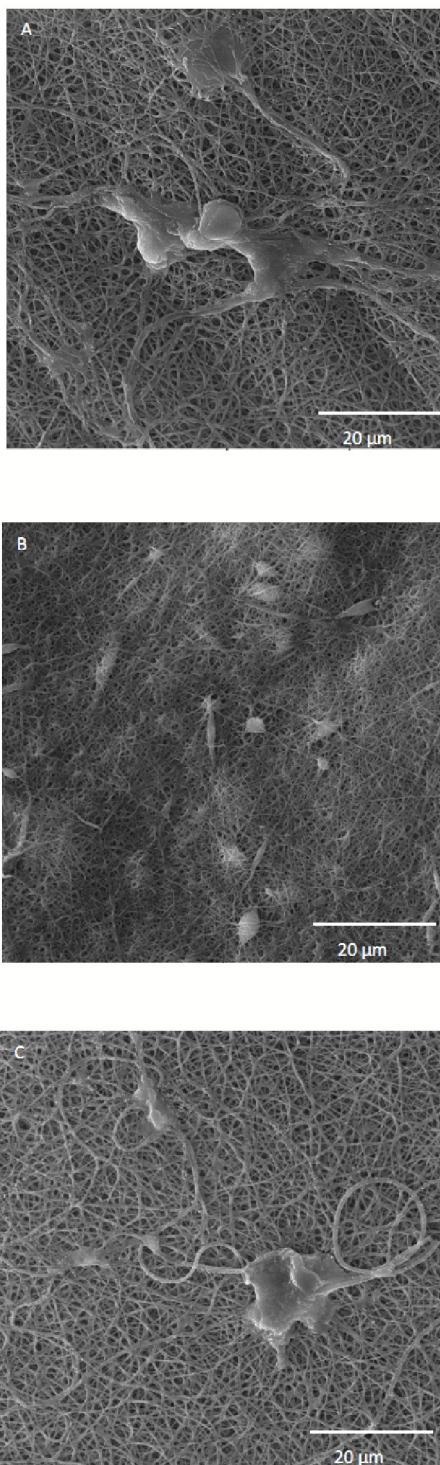Achievement of a uniform bead-free morphology is important in the electrospinning of nanofibers. Deng et al [18] have prepared chitosan/PVA nanofibers containing organic rectorites but the morphologies of the electrospun mats were not as uniform as the nanofibrous mats prepared in this study. Results of SEM/EDX in this study showed that nanolayers of MMT were distributed uniformly inside the nanofibers. One of the reasons of achieving this result may be explained by the fact that in the electrospinning process, a strong elongational force is applied to the solution which enhances the distribution of the MMT nanoclays in the nanofibers. Moreover, NH_2 groups of chitosan protonate into NH_3^+ in acidic media and a cation exchange reaction can take place between the negatively charged surfaces of nanoclays and the charged groups of chitosan chains [25]. Since this is a thermodynamically favorable reaction [1], it leads to the exfoliation of nanoclays.

Results of X-ray studies in the previous works stated that MMT nanoclays were intercalated. In the present work, it is shown that MMT nanoclays were exfoliated. In this regard, the method of preparation of the electrospinning solutions is notable. We prepared MMT dispersion in water and allowed to stir for 3 days at 50 °C to reach a completely exfoliated dispersion and the prepared dispersion was added to the chitosan/PVA solutions. Other works prepared the same dispersion with stirring in a shorter time period (2-4 hours)[20, 21].

In our previous study, nanocomposite films from chitosan/PVA and MMT nanoclays were prepared for wound dressing applications [16]. Although the nanocomposite films possess acceptable mechanical properties for using in many biomedical applications, they lack sufficient porosity which is essential for specific applications such as tissue engineering scaffolds[26]. On the contrary, nanofibrous mats have a highly porous structure compared to the films which in addition to their similarity to the natural extra

17

cellular matrix, makes them appropriate materials to be used as tissue engineering scaffolds [27].

Interestingly, in the present work, it was shown that MMT nanoclays were successfully incorporated in

chitosan/PVA nanofibers (figure 2) which could enhance mechanical properties of the mats (Table 2).

Regarding to mechanical properties of mats, the tensile strength of the nanofibrous mats containing 1%

and 3% MMT prepared in our work was about 15.45 and 15.10 MPa, respectively which is higher than

the values achieved in the previous studies [17]. It is well known that dispersion of nanoparticles inside the

polymer matrices play an important role in improving the physical and mechanical properties of

nanocomposites [4]. Uniform unbeaded morphology observed in the SEM micrographs of this study may

be one of the reasons of achieving high values of tensile strength, because beads can act as local stress

concentrators and reduce the strength of the mats.

The glass transition of chitosan has been subject of controversy. Sakurai et al [24] has reported the glass

transition of chitosan to be 203°C after the second heating run by DSC and DMTA methods, while other

researchers suggest that the glass transition of chitosan is higher than its decomposition temperature and

cannot be detected [28]. We did not detect the glass transition of the as-received chitosan from Its DSC

thermogram. In the case of PVA, the glass transition temperature is detected to be 56°C. This value is

slightly lower than other values reported in the literature for PVA [29]. The reason may be due to the lower

molecular weight and moisture absorption of the PVA used in this study. The glass transition temperature

of the blends of CS/PVA and CS/PVA/MMT 1% are observed near the value of the pure PVA. However,

the glass transition peak is not observed for CS/PVA/MMT 3%. This result may be due to the restriction

of molecular motions of PVA chains caused by the presence of MMT nanolayers. This is supported by

comparing the results of dynamic mechanical behavior and DSC thermograms. In figure 6.b we observe

a shoulder near 50°C in the tan delta curve for the CS/PVA and CS/PVA/MMT 1% mats while this peak

is not observed in the curve of CS/PVA/MMT 3%.

As mentioned in the introduction, Xin and coworkers [21] reported that OREC can induce cytotoxicity to the nanocomposite mats of carboxymethyl chitosan/PVA/OREC. The results of this study showed that chitosan/PVA/MMT nanofibrous mats have less cytotoxicity and are more biocompatible than the organic rectorites. It can be concluded that unmodified MMT nanoclays, in addition to improving the physical and mechanical properties of the mats, are less cytotoxic and are more promising nanoparticles to be used with hydrophilic polymers for biomedical applications.

4 Experimental

4.1 Materials

Chitosan (low viscosity, degree of deacetylation 92% determined by FT-IR) was purchased from Fluka. Poly (vinyl alcohol) with molecular weight of about 89000-98000 g/mol and 98% degree of hydrolysis, was provided by Sigma Aldrich. Unmodified natural montmorillonite nanoclay (Cloisite Na$^+$, Southern Clay Products Incorporation) was used for preparation of solutions containing MMT. Mixture of double distilled water and glacial acetic acid (Merck) in 30/70 volume ratio was used as solvent for preparation of electrospinning solutions. RPMI 1640, fetal bovine serum, penicillin/streptomycin, L-glutamine, phosphate buffer saline (PBS) were purchased from GIBCO company. Additionally, 3-(4,5-dimethylthiazol-2-yl)-2,5-diphenyl tetrazoliumbromide (MTT), dimethyl sulfoxide (DMSO), ethanol and glutaraldehyde were obtained from Merck company.

4.2 Solutions preparation

1400 mg chitosan was dissolved in 20 cc solvent by magnetic stirring overnight to prepare 7 wt% solutions. 7 wt% PVA solutions were prepared by the same method while the temperature was raised to 80°C for 2 hours to enhance dissolution of PVA crystals. Chitosan and PVA solutions were mixed to prepare 20 cc solution with chitosan/PVA volume ratio of 30/70.

In order to incorporate MMT into the solutions, a stock solution containing 1 g of MMT dispersed into 100 ml acetic acid (70%) was prepares and vigorously stirred for 72 hours at 50°C to exfoliate the nanolayers. Predetermined volume of this solution was added to the chitosan/PVA solutions to reach 1% and 3% nanoclay (per weight of solid polymer) and allowed to stir overnight. The electrospun samples from the solutions are noted as CS/PVA, CS/PVA/MMT 1% and CS/PVA/MMT 3% throughout the text.

4.3 Electrospinning

The solutions were electrospun immediately after preparation. A glass syringe filled with the electrospinning solution was placed in the holder which was moved by the pump to produce a constant injection rate. The solution flows from the syringe to a silicone tube connector, passes through the stainless steel needle (G18, inner diameter 0.84 mm) and enters the electric field which is provided by an adjustable high voltage supply. The device is provided with exhausting fans to evaporate the solvents and the remaining polymer chains forming the nanofibrous mats are collected on the aluminum foil covered on the rotating mandrel. The mandrel can rotate with a tunable speed. All process parameters such as needle tip to collector distance (TCD), injection rate, rotation speed of mandrel, scan position of the needle and the electric field are adjusted and controlled by a digital screen.

Electrospinning of prepared solutions was performed at room temperature, voltage of 20 kV and injection rate of 0.1 ml/h. TCD was set to 100 mm for all samples and the collector rotated with a speed of 700 rpm. The nanofibers collected on aluminum foils were covered and stored at room temperature for the rest of characterization tests.

4.4 Characterization of nanofibers

4.4.1 Fourier transforms infrared spectroscopy (FTIR)

FTIR spectra of the nanofibers were recorded by ABB (formerly Bomem) spectrometer in transmission mode. The nanofibers were rubbed and mixed with KBr powder in a weight ratio of 1/100 and mechanically pressed to form a clear disc and placed in the holder in front of the beam. FTIR spectra of the samples was achieved by 20 scans in the range of $400\text{-}4000\ cm^{-1}$ with a resolution of $2\ cm^{-1}$.

4.4.2 Scanning electron microscopy and energy dispersive X-ray scattering (SEM/EDX)

Morphologies of the resulting nanofibers were studied by SEM (VEGA\\TESCAN, Czech Republic) in the magnification of 10 K after coating with gold. Average diameters of nanofibers were measured by Image-Pro plus 6.0 software. In order to map the distribution of nanoclays into the nanofibers, spot analysis was performed by an energy dispersive X-ray analyzer (INCA, Oxford instruments, England) connected to the SEM. As nanoclays are aluminosilicate nanolayers, Si atom was mapped to visualize the distribution of nanoclays inside the nanofibers.

4.4.3 Small angle X-ray diffraction (SAXRD)

Small Angle X-ray diffraction (SAXRD) spectra of nanocomposite nanofibers was recorded by a XPERT type diffractometer (X'Pert MPD, Philips Analytical, The Netherlands) using Co tube anode with a wavelength of $\lambda=0.179$ nm in the range of $1.01°$ to $11.9°$ by a step size of .02.

4.4.4 Differential scanning calorimetry (DSC)

DSC analysis was conducted under nitrogen atmosphere by Mettler Toledo Differential Scanning Calorimeter. In order to determine the effects of electrospinning on thermal behavior of the chitosan and PVA, these polymers have been tested before and after electrospinning. At least 5 mg of each sample was weighted, sealed in aluminum pans and heated from 25 °C to 300 °C by a heating rate of 10 °C/min. The reference material was an empty pan. Baseline inflection point was taken as glass-rubber transition

temperature (T_g) and temperature of the endothermic peak during heating was taken as melting point (T_m) of the samples.

4.5 Mechanical Properties

4.5.1 Dynamic mechanical thermal analysis (DMTA)

The specimens for the DMTA test were rectangular samples cut from the nanofibrous mats into the dimensions of 1×3 cm with a thickness of 0.01 mm measured by a digital micrometer. DMTA experiments were performed in tension mode using a TTDMA dynamic mechanical analyzer (Triton Technology Incorporation). The length of the sample between the grips was 5 mm and the displacement was set to 0.005 mm (1% of the length between grips) and the frequency was constant at 1 Hz to be in the linear viscoelastic range. The temperature sweep was conducted on the samples from room temperature (25°C) up to 160°C with a rate of 5 °C/min.

4.5.2 Tensile strength

Stress-strain curves of nanofibrous mats were measured according to ASTM D882-12 (2012) using a single column universal testing machine (Tinius Olsen H1KS, SDL ATLAS, USA) with a 1 kN load cell. The specimens were carefully peeled off from aluminum foil and cut into strips of 0.5×5 cm and a gauge length of 20 mm was considered. The samples were mounted into the grips and stretched with a strain rate of 10 mm/min until breakage. Five samples of each formulation was tested and averages of Young's modulus of elasticity (E), ultimate tensile strength (UTS) and elongation at break (ε_b) were evaluated from stress-strain curves. The toughness of the specimens was calculated by integrating the area under the stress-strain curves.

4.6 *in vitro* cytotoxicity by MTT assay

At first, the mats were heated to 80°C for 2 hours in a vacuum oven (Memmert, Germany) to be stabilized in aqueous media. The samples were cut into rectangular shapes of 2 cm x1 cm, immersed into ethanol 70% (containing 30% NaOH 0.1 M) for 30 minutes to neutralize the remaining acetic acid and also to be disinfected. Then, samples were washed with sterilized PBS for 3 times. Cytotoxicity of the mats was evaluated by indirect contact MTT assay based on a procedure from the ISO 10993-5 standard test method [30]. The samples were prepared according to ISO 10993-12 standard test method [31]. Approximately 4 cm^2 of each sample was immersed in 2 ml of serum-free culture medium (RPMI 1640 containing 1 vol.% L-glutamine and 1 vol.% penicillin and streptomycin as antibiotics) for 1, 3 and 6 days at 37°C. The serum-free culture medium without nanofibers was also incubated at 37°C in the mentioned times and used as control. The A-431 cell line was obtained from national cell bank of Iran, Pasteur institute of Iran, Tehran, Iran. The cells were cultured in a 96-well plate at a density of 1×10^4 cells per well and 100 μL of RPMI 1640 supplemented by 10% FBS was added to each well and incubated for 24 hours (37°C, 99% RH, 5% CO_2) . A number of 6 replicates were considered for each sample. After that, the culture medium was replaced by the prepared extracts followed by addition of 1 μL FBS to each well. After 24 hours incubation, the extract solutions were removed and 100 μL MTT solution (0.5 mg/mL in PBS) was added to each well and incubated for 4 hours. Finally, the MTT solution was removed and 100 μL DMSO was added to each well followed by incubation for 15 minutes. Absorbance at 570 nm was read by ELISA microplate reader (Awareness Technology Incorporation). The relative cell viability of the control media were defined as 100% and cell viabilities for the samples was calculated relative to the control value.

23

4.7 Cell attachment study

To study the attachment of the cells on the surface of nanofibrous mats, the A-431 cells with a density of 5×10^4 cells/sample were seeded in a 24-well plate containing the sample at the bottom of the well supplemented by 2 ml of RPMI 1640 with 10% FBS. The plates were incubated at 37°C and 5% CO_2 for 24 hours. Subsequently, the samples were fixed with 2.5% glutaraldehyde solution for 2 hours followed by washing with PBS and dehydrating with 30%, 50% 75%, 95% and absolute ethanol. The samples were dried and used for SEM observation.

4.8 Mathematical and statistical analyses

All of the quantitative data were represented by means ± standard error. The mathematical calculations and graphing were performed using MATLAB (R2013a) software. The means of optical densities from MTT assay data and also the values represented for the mechanical properties were statistically examined by the one-way analysis of variance (ANOVA) followed by post hoc Tukey's test (IBM SPSS Statistics, version 22.0). The p-values lower than 0.05 were considered as significant.

5 Conclusions

In this work, it is shown that chitosan/PVA/MMT nanofibers can be produced without beaded morphology by the method used in this study. The results of SAXRD showed that MMT nanoclays were exfoliated. The mechanical properties of the nanocomposite nanofibers are highly improved by addition of only 1 and 3 wt.% MMT. Presence of MMT nanoclays reduced the damping of the nanofibrous mats and increased the maximum damping to higher temperatures. The molecular chain motion of the PVA polymers was restricted by addition of MMT nanoclays and the glass transition of PVA was not detected in the DMTA curves for the sample containing 3% MMT. This result is supported by the DSC thermograms. Apart from the improvement of physical and mechanical properties, MMT nanoclays are

more biocompatible nanoparticles and show less cytotoxicity to fibroblast cells. Therefore, it is suggested that electrospun nanocomposite nanofibers of chitosan/PVA/nanoclays are favorable materials for bio-applications.

6 References

1. K. Kabiri, H. Mirzadeh and M. J. Zohuriaan-Mehr, *Iranian Polymer Journal*, 2007, **16**, 147.
2. H. Azizi, J. Morshedian, M. Barikani and M. Wagner, *Express Polym. Lett.*, 2010, **4**, 252-262.
3. M. Kokabi, M. Sirousazar and Z. M. Hassan, *Eur. Polym. J.*, 2007, **43**, 773-781.
4. L. A. Utracki, *Clay-containing polymeric nanocomposites. 1*, iSmithers Rapra Publishing, 2004.
5. D. Li and Y. Xia, *Adv. Mater.*, 2004, **16**, 1151-1170.
6. S. Ramakrishna, *An introduction to electrospinning and nanofibers*, World Scientific Publishing Company, Singapore, 2005.
7. E. A. T. Vargas, N. C. do Vale Baracho, J. de Brito and A. A. A. de Queiroz, *Acta Biomater.*, 2010, **6**, 1069-1078.
8. S. S. Ojha, D. R. Stevens, T. J. Hoffman, K. Stano, R. Klossner, M. C. Scott, W. Krause, L. I. Clarke and R. E. Gorga, *Biomacromolecules*, 2008, **9**, 2523-2529.
9. M. A. Shokrgozar, F. Mottaghitalab, V. Mottaghitalab and M. Farokhi, *J. Biomed. Nanotechnol.*, 2011, **7**, 276-284.
10. H. Liao, R. Qi, M. Shen, X. Cao, R. Guo, Y. Zhang and X. Shi, *Colloids Surf. B. Biointerfaces*, 2011, **84**, 528-535.
11. S. I. Marras, K. P. Kladi, I. Tsivintzelis, I. Zuburtikudis and C. Panayiotou, *Acta Biomater.*, 2008, **4**, 756-765.
12. R. Jayakumar, M. Prabaharan, S. V. Nair and H. Tamura, *Biotechnol. Adv.*, 2010, **28**, 142-150.
13. E. Mirzaei, R. Faridi-Majidi, M. A. Shokrgozar and F. Asghari Paskiabi, *Nanomedicine Journal*, 2014, **1**, 137-146.
14. F. Mottaghitalab, M. Farokhi, V. Mottaghitalab, M. Ziabari, A. Divsalar and M. A. Shokrgozar, *Carbohydr. Polym.*, 2011, **86**, 526-535.
15. Y. Xu, X. Ren and M. A. Hanna, *J. Appl. Polym. Sci.*, 2006, **99**, 1684-1691.
16. H. Mahdavi, H. Mirzadeh, M. J. Zohuriaan-Mehr and F. Talebnezhad, *J. Am. Sci.*, 2013, **9**, 203-214.
17. J. Park, H. Lee, D. Chae, W. Oh, J. Yun, Y. Deng and J. Yeum, *Colloid Polym. Sci.*, 2009, **287**, 943-950.
18. H. Deng, X. Li, B. Ding, Y. Du, G. Li, J. Yang and X. Hu, *Carbohydr. Polym.*, 2011, **83**, 973-978.
19. B. Liu, X. Wang, C. Pang, J. Luo, Y. Luo and R. Sun, *Carbohydr. Polym.*, 2013, **92**, 1078-1085.
20. H. Deng, P. Lin, S. Xin, R. Huang, W. Li, Y. Du, X. Zhou and J. Yang, *Carbohydr. Polym.*, 2012, **89**, 307-313.
21. S. Xin, Y. Li, W. Li, J. Du, R. Huang, Y. Du and H. Deng, *Carbohydr. Polym.*, 2012, **90**, 1069-1074.
22. B. Narayan, *J. Nanomedic. Biotherapeu. Discover.*, 2012, **2**, 102-111.
23. J. Brugnerotto, J. Lizardi, F. Goycoolea, W. Argüelles-Monal, J. Desbrieres and M. Rinaudo, *Polymer*, 2001, **42**, 3569-3580.
24. K. Sakurai, T. Maegawa and T. Takahashi, *Polymer*, 2000, **41**, 7051-7056.
25. K.-F. Lin, C.-Y. Hsu, T.-S. Huang, W.-Y. Chiu, Y.-H. Lee and T.-H. Young, *J. Appl. Polym. Sci.*, 2005, **98**, 2042-2047.
26. B.-S. Kim, I.-K. Park, T. Hoshiba, H.-L. Jiang, Y.-J. Choi, T. Akaike and C.-S. Cho, *Prog. Polym. Sci.*, 2011, **36**, 238-268.
27. J. Lin, X. Wang, B. Ding, J. Yu, G. Sun and M. Wang, *Crit. Rev. Solid State Mater. Sci.*, 2012, **37**, 94-114.

28.   F. S. Kittur, K. V. Harish Prashanth, K. Udaya Sankar and R. N. Tharanathan, *Carbohydr. Polym.*, 2002, **49**, 185-193.

29.   E. Parparita, N. Cheaburu and C. Vasile, *Cellulose Chem. Technol*, 2012, **46**, 571-581.

30.   B. ISO, *Tests for in vitro cytotoxicity*, 2008.

31.   E. ISO, *German version: DIN EN ISO*, 2008, 10993-10912.